

Synthesis of and Studies on 4-Methylpiperazine-1-carbamic Acid and Morpholinecarbamic Acid Complexes of Copper(II)

Shashi B. Kalia, Rajesh Kumar, Monika Bharti and Poonam Sharma
Department of Chemistry, Himachal Pradesh University Shimla-171005 India

Abstract: New 4-methylpiperazine-1-carbamic acid (4-MPipzcbmH) and morpholinecarbamic acid (MorphcbmH) complexes of copper(II) of the general formula $Cu(L)_2X_2$ ($L = 4\text{-MPipzcbmH}$ and $MorphcbmH$; $X = CH_3COO$ and $X_2 = SO_4$) have been synthesised and investigated by elemental analysis, molar conductance, thermogravimetric analysis (TGA), infrared, fluorescence, mass, and solution electronic absorption spectral studies. Room temperature magnetic susceptibility measurements, XRD and cyclic voltametric studies have also been performed. The complexes are paramagnetic corresponding to copper(II), a d^9 system. The ligands 4-MPipzcbmH and MorphcbmH and their copper(II) complexes have also been screened against the lipase enzyme for assaying their enzyme activity.

Keywords: 4-Methylpiperazine-1-carbamic acid and Morpholinecarbamic acid, Copper(II), Fluorescence, Cyclic voltammetry

I. Introduction

Carbamates represent important building blocks in natural products, agrochemicals, and pharmaceutical drugs.^{1,2} They play a significant role in organic chemistry as starting materials, intermediates, and protecting groups.³ Carbamates are generally prepared by employing chloroformates, isocyanates, and phosgene.^{4,1a} The combination of carbon dioxide, water, and metal catalysts was introduced as a substitute for the toxic phosgene.^{5,1a} Carbamate compounds containing the group $^-O_2CNR_2$ act as ligands which may have donor atoms either oxygen, or both oxygen and nitrogen. They belong to the 1,1-dioxo chelating class of compounds and are derived from carbamic acid, H_2NCO_2H . Carbamic acid, monoamide of carbon dioxide constitutes the backbone of carbamate structure. Carbamic acid H_2NCO_2H and its derivative containing the carbon dioxide fragment are thermally unstable and structural characterization and isolation of the dibenzyl derivative Bz_2NCO_2H is quite recent. Carbamates vary in their spectrum of activity, mammalian toxicity and persistence. They are relatively unstable compounds that break down in the environment within weeks or months. Carbamates are commonly used as surface sprays or baits in the control of household pests. Carbamate complexes of non-transition elements have been mostly prepared by carbonation of readily available corresponding amides. While transition element carbamates required more sophisticated preparative routes. Copper carbamate complexes are found to exist mainly in +1 and +2 oxidation states of copper. Copper(II) was found to be solvent extracted from aqueous solution of $CuSO_4$ in presence of a secondary amine NHR_2 (R should be a primary alkyl group such as butyl or benzyl) under carbon dioxide, similar to extraction of metal cations from aqueous solution into hydrocarbons by the NHR_2/CO_2 system. Some copper(II) carbamates wherein carbamates have been derived from saturated heterocyclic secondary amines, 1-methylpiperazine and morpholine have been synthesised and investigated.

II. Experimental

Material and Methods

All the chemicals used were of analytical reagent grade and used as such.

Preparation of Ligands

4-Methylpiperazine-1-carbamic Acid (4-MPipzcbmH) and Morpholinecarbamic acid (MorphcbmH):

The free ligands 4-MPipzcbmH and MorphcbmH were obtained by the method as given in the procedure reported for patent.^{6a}

Preparation of Metal Carbamate Complexes

1) $Cu(4\text{-MPipzcbmH})_2(CH_3COO)_2$, $Cu(MorphcbmH)_2(CH_3COO)_2$

Solid 4-methylpiperazine-1-Carbamic acid (144.24 mg, 1.000 mmol) or morpholinecarbamic acid (131.22 mg, 1.000 mmol) was added in small portions (10 mg) after successive intervals of 15-20 minutes in a total period of about 4 hours to a continuously stirred benzene solution (5 ml) of 100 mg (0.500 mmol) of cupric acetate $Cu(CH_3COO)_2 \cdot H_2O$ kept at 25-30°C. Green coloured complex $Cu(4\text{-MPipzcbmH})_2(CH_3COO)_2$ and light purple coloured complex of $Cu(MorphcbmH)_2(CH_3COO)_2$ were obtained. The reaction mixture was stirred

for another one hour. Complex thus formed was centrifuged, washed with benzene using centrifugation technique and then dried in air. Final drying of sample was done by keeping it overnight in a calcium chloride desiccator.

2) $\text{Cu(4-MPipzcbmH)}_2\text{SO}_4$, $\text{Cu(MorphcbmH)}_2\text{SO}_4$

Methanolic solution (5ml) of $\text{CuSO}_4 \cdot 5\text{H}_2\text{O}$. (86.70 mg, 0.347 mmol for 4-methylpiperazine-1-carbamic acid or 95.31 mg, 0.381 mmol for morpholinecarbamic acid) was prepared. To it was added with stirring 100mg of solid 4-methylpiperazine -1-carbamic acid (0.694mmol) or morpholinecarbamic acid (0.763 mmol) in small portions (10mg) after successive intervals of 15-20 minutes in a total period of about 3 hours. The reaction was carried out at 25-30 °C .A solid sky blue coloured product was obtained .It was centrifuged ,washed with methanol using centrifugation technique and dried in air. Final drying of the sample was done by keeping it overnight in a calcium chloride dessiccator.

Elemental analyses

Carbon and hydrogen analyses were performed on an automatic Coleman-33 Analyser, while nitrogen was analysed by Kjeldahl's method. Sulphur was determined gravimetrically as barium sulphate. Copper was estimated volumetrically by EDTA using Pyrocatechol violet indicator.

$\text{Cu(4-MPipzcbmH)}_2(\text{CH}_3\text{COO})_2$ Analysis found: C 40.84, H 6.42, N 11.88, Cu 13.55, CH_3COO 25.10%; Calculated for $\text{CuC}_{16}\text{H}_{30}\text{N}_4\text{O}_8$: C 40.89, H 6.38, N 11.92, Cu 13.52, CH_3COO 25.13%. Reaction yield 85%. Decomposition temperature: 156 °C.

$\text{Cu(4-MPipzcbmH)}_2\text{SO}_4$ Analysis found: C 32.22, H 5.38, N 12.55, S 7.11, Cu 14.22,%; Calculated for $\text{CuC}_{12}\text{H}_{24}\text{N}_4\text{O}_8\text{S}$: C 32.17, H 5.36, N 12.51, S 7.15, Cu 14.18%. Reaction yield 83%. Decomposition temperature: 147 °C.

$\text{Cu(MorphcbmH)}_2(\text{CH}_3\text{COO})_2$ Analysis found: C 37.91, H 5.39, N 6.29, Cu 14.35, CH_3COO 26.56%; Calculated for $\text{CuC}_{14}\text{H}_{24}\text{N}_2\text{O}_{10}$: C 37.88, H 5.41, N 6.31, Cu 14.31, CH_3COO 26.60%. Reaction yield 84%. Decomposition temperature: 108 °C.

$\text{Cu(MorphcbmH)}_2\text{SO}_4$ Analysis found: C 28.51, H 4.30, N 6.60, S 7.62, Cu 15.10,%; Calculated for $\text{CuC}_{10}\text{H}_{18}\text{N}_2\text{O}_{10}\text{S}$: C 28.46, H 4.27, N 6.64, S 7.59 Cu 15.06% . Reaction yield 88%. Decomposition temperature: 115 °C.

Physical measurements

Molar conductance measurements (10^{-3} M DMSO solutions) were made at room temperature using Elico Conductivity Bridge type CM-82T. Thermal analyses of the complexes were carried out on thermogravimetric analyzer (TGA)-Model 2950, Make-TA Instruments, USA and differential scanning calorimeter (DSC)—Model 2920, Make—TA Instruments, USA. The thermocouple used was Pt/Pt–Rh (10 %) with a temperature range of 20–800°C. Infrared spectra of complexes were recorded as KBr pellets on Nicolet 5700 FT Infrared Spectrophotometer in the 4000-600 cm^{-1} region. While for 600 – 200 cm^{-1} spectra were recorded as NaCl plates as windows. Fluorescence emission spectra of compounds were recorded on 10^{-3} M DMSO solution using Perkin Elmer LS 55 spectrometer with scanning range from 200-900 nm. Mass spectra of complexes was recorded on an Agilent LCMS (6300) Ion-Trap mass spectrometer (mass range: 80-2200 m/z). Sample dissolved in DMSO (2 mg/10 ml) was introduced into Electron spray ionization (ESI) source through MS injection, using infusion method. Magnetic susceptibilities of the samples were measured on a Vibrating Sample Magnetometer PAR-155 (model-152) at the Institute Instrumentation Centre (IIC) of Indian Institute of Technology, Roorkee. The instrument was calibrated with $\text{Cu(OOCCH}_3)_2 \cdot \text{H}_2\text{O}$, whose magnetic susceptibility at room temperature is known. Solution (DMSO) electronic absorption spectra of complexes, with solvent as reference, in quartz glass cells were recorded on Cary 100 Bio UV-Visible recording Spectrophotometer (range 200-900 nm) and Analytikjena Specord 200 UV-Visible recording Spectrophotometer (range 1100-200 nm). PXRD patterns were obtained using Bruker AXSd8 advance X-ray diffractometer with Mo-K_α ($\lambda = 0.7107 \text{ \AA}$) and Cu-K_α ($\lambda = 1.54184 \text{ \AA}$) radiation sources. The measurements were made at a temperature of 25 °C (RT) and a 2θ angle range of 10°-80°. A step resolution of 0.019° was used with a step time of 19.2 s. Cyclic voltammograms of compounds in DMSO solution (10^{-3} M) using KCl/ NaClO_4 (10^{-1} M) as supporting electrolyte in the potential range -2 to +2 V at a scan rate of 100 mV sec^{-1} were recorded on Autolab Potentiostat 128N Electrochemical Analyzer with potential scanning range from + 10 to -10 Volts.

Lipase Enzyme Activity

In present study compounds were also tested for the lipase enzyme (steapsin) activity at different incubation times between 0 to 70 minutes. All the experiments were performed in triplicate. The lipase enzyme inhibition activity of compounds alongwith control was recorded after 10, 30, 50, and 70 minutes. In six dry and clean test tubes labelled A,B,C,D,E,F trisbuffer gum acacia solution (2.90 ml,0.05 M,pH 8.5) was taken.These

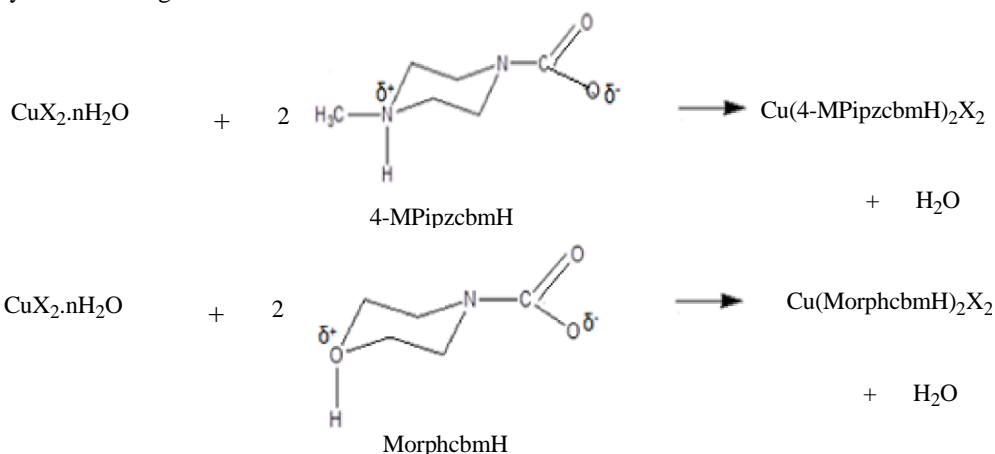
were incubated in water bath at 45°C for 10 minutes, removed from the water bath and cooled to room temperature. Eighty microliter (80µl) of p-nitrophenyl palmitate (p-NPP) substrate solution was added to each test tube which were again incubated in water bath at 45°C for another 10 minutes. In another set of four clean and dry test tubes was taken 1mg of solid compound under study. Added 10 µl of steapsin lipase enzyme in each of these test tubes. The test tubes were numbered as 1,2,3,4 and were incubated at 45°C on water bath for 10,30, 50 and 70 minutes respectively. All the experiments were performed in triplicate. In another one clean and dry test tube 10 µl of steapsin lipase enzyme was taken and added the solution of test tube marked A into it. Then again incubated the test tube in water bath at 45°C for 10 minutes. The enzyme activity was arrested by keeping the reaction mixture at -80°C for about 5 minutes. Then A_{410nm} of the solution was measured. Added the solutions of test tubes B,C,D,E into test tubes 1,2,3,4 after 10 ,30,50 and 70 minutes respectively., Test tubes were incubated in water bath at 45°C for 10 minutes. . The enzyme activity was arrested by keeping the reaction mixture at -80°C for about 5 minutes. Then A₄₁₀ of the solution was measured. The activity of enzyme was calculated with the help of formula

Activity of enzyme

$$= \frac{\text{Test}(t) - \text{Control}(C)}{\text{OD of Standard}} \times \text{Conc. of standard} \times \frac{1}{10} \times \text{Dilution factor} \times \frac{1}{\text{Molecular weight of p - NPP}}$$

III. Results And Discussion

Cu(4-MPipzcbmH)₂X₂ , Cu(MorphcbmH)₂X₂ (X = CH₃COO⁻ and X₂ = SO₄²⁻) complexes were prepared by the following reactions



where X = CH₃COO⁻ when n=1 and X₂ = SO₄²⁻ when n = 5

These complexes do not melt but decompose between 108°C -156°C and are sparingly soluble in methanol and ethanol but are fairly soluble in DMSO.

Molar conductance studies

The 10⁻³ M DMSO solution of complexes Cu(4-MPipzcbmH)₂SO₄ and Cu(MorphcbmH)₂SO₄ exhibit molar conductance values 20 ohm⁻¹cm²mol⁻¹ and 19 ohm⁻¹cm²mol⁻¹ respectively suggesting their non-electrolytic nature. Whereas Cu(4-MPipzcbmH)₂(CH₃COO)₂ and Cu(MorphcbmH)₂(CH₃COO)₂ complexes show molar conductance values 146 ohm⁻¹cm²mol⁻¹ and 172 ohm⁻¹cm²mol⁻¹ respectively that support their 1:2 electrolytic behaviour

Thermal studies

TG/DSC curve of Cu (MorphcbmH)₂(CH₃COO)₂ complex shows it decomposing in four steps (Figure-1,2). First step involves the elimination of two moles of acetic acid at a temperature of 65- 115°C with mass loss of 27.08% . Second step occurs at a temperature of 160 - 180°C with mass loss of 19.25% corresponding to loss of one mole of amine, i.e. morpholine . Third step involves removal of carbon dioxide molecule with mass loss of 9.98% between 180 – 220°C. Last step involves elimination of one mole each of morpholine and carbon monoxide with total mass loss of 25.50% between 220- 280°C (Table-1) . Species left as residue(18.1%) is CuO. DSC curve shows two endothermic peaks for first step at 80°C and 120°C , second step shows endothermic peak at 176°C . Fourth step is exothermic occurring at 275°C .

A perusal of TG/DSC curves of complex $\text{Cu}(\text{MorphcbmH})_2\text{SO}_4$ is indicative of four step decomposition pattern(Figure-3,4) . First stage decomposition in the temperature range $40 - 95^\circ\text{C}$ corresponding to a mass loss of 15.10% has revealed a loss of one mole of sulphur dioxide . Second step occurs at a temperature of $165 - 205^\circ\text{C}$ with mass loss of 16.20% corresponding to loss of one mole of H_2 and two moles of oxygen (O_2). Third step decomposition involves elimination of four moles of ethylene, one mole of nitrogen (N_2) and one mole of carbon monoxide between $205 - 325^\circ\text{C}$ with a total mass loss of 39.95%. Fourth step follows elimination of one mole of carbon dioxide between $325 - 575^\circ\text{C}$ with mass loss of 10.35% . Residue, 18.17% corresponds to CuO (Table-1). DSC curve of complex shows three endothermic peaks at 60°C , 199°C and 270°C corresponding to first, second and third step respectively(Figure-4).

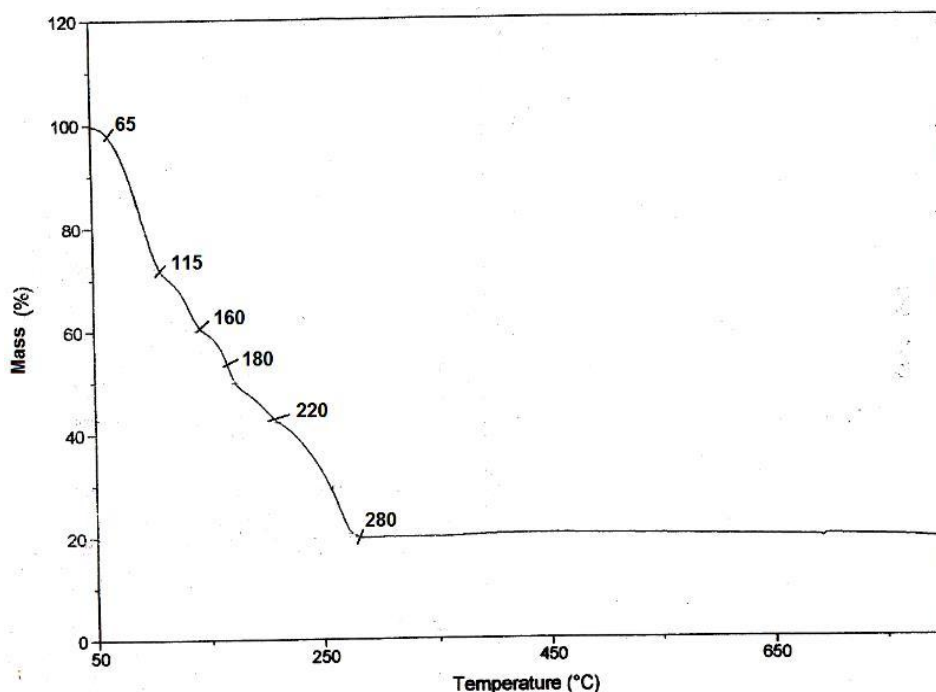


Figure-1 TG curve of $\text{Cu}(\text{MorphcbmH})_2(\text{CH}_3\text{COO})_2$

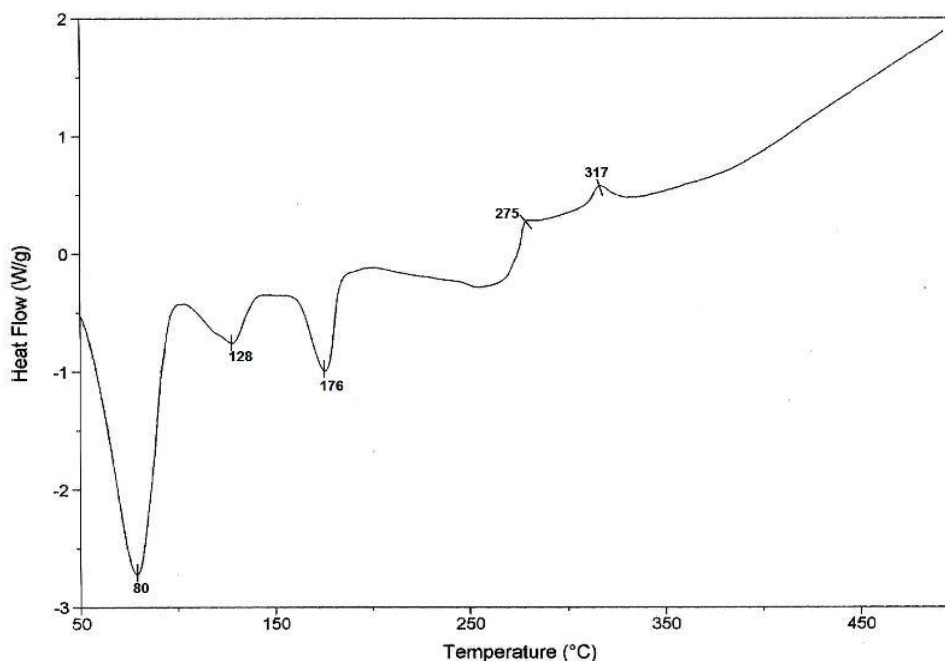


Figure-2 DSC Curve of $\text{Cu}(\text{MorphcbmH})_2(\text{CH}_3\text{COO})_2$

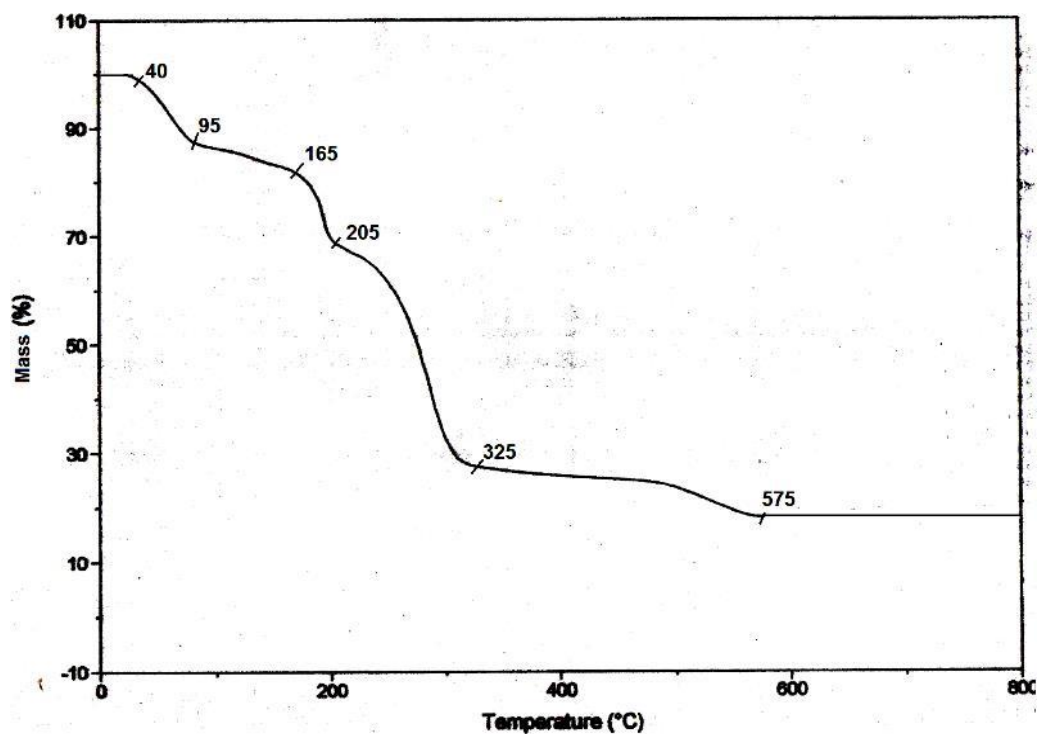


Figure-3 TG Curve of $\text{Cu}(\text{MorphcbmH})_2\text{SO}_4$

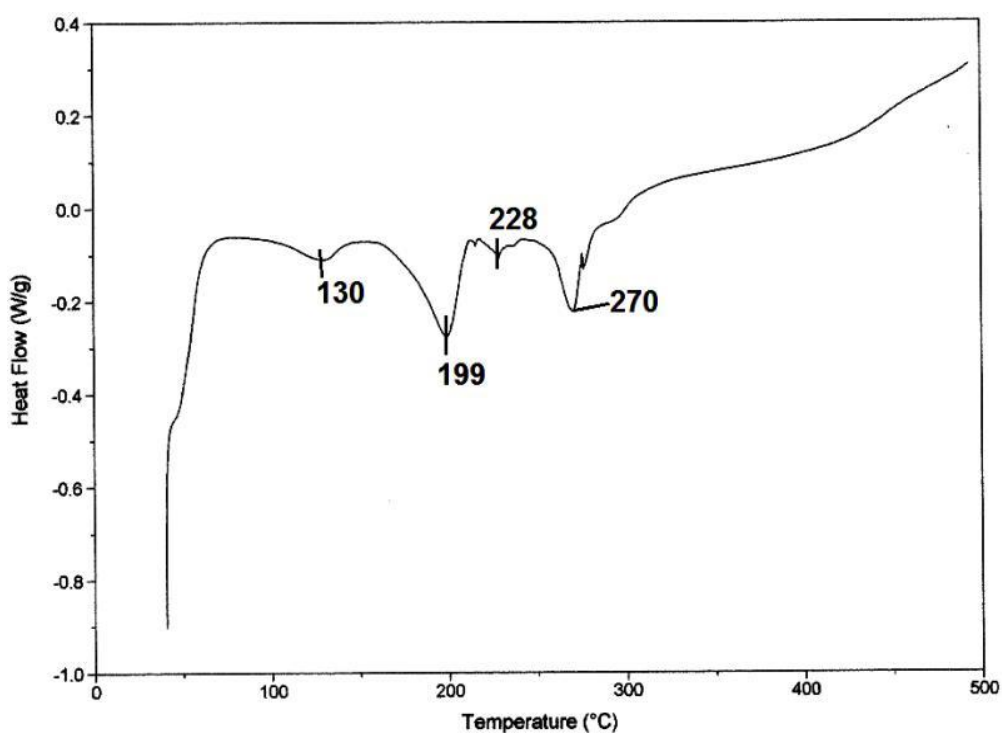
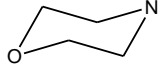


Figure-4 DSC Curve of $\text{Cu}(\text{MorphcbmH})_2\text{SO}_4$

It has been observed that for TG/DSC patterns for the complexes under investigation experimental percent mass loss matches with the corresponding theoretical percent mass loss (Table-1) for their various stages of thermal decomposition which supports present thermal decomposition pattern is in relevance to literature reports.^{6b}

Table -1 Thermal Decomposition Data of Cu(MorphcbmH)₂(CH₃COO)₂ and Cu(MorphcbmH)₂SO₄

Sr. No.	Compound Mol. Wt.	Sample Mass /mg	Initial Dec. Temp / °C	Stage s of Dec.	TG Temp. / °C	Mass Loss% (Mol. Wt.) Exp. Theo.	Theor. Mass Left / % Mol Wt.	Species Lost	Species Formed	DSC Peak / °C	Nature
1.	Cu(MorphcbmH) ₂ (CH ₃ COO) ₂ 443.5	10.56	65	1 st	65-115	27.08 27.05 (120.11) (120)	72.95 (323.16)	2 CH ₃ COOH	Cu(MorphcbmH) ₂	80,128	Endo, Endo
				2 nd	160-180	19.25 19.39 (85.37) (86)	53.56 (237.27)		Cu(MorphcbmH)(CO ₂)	176	Endo
				3 rd	180-220	9.98 9.92 (44.3) (44)	43.64 (193.32)	CO ₂	Cu(Morphcbm)	-	-
				4 th	220-280	25.50 25.70 (113.09) (114)	18.1 (80.18)		CuO	275	Exo
2.	Cu(MorphcbmH) ₂ SO ₄ 421.5	11	40	1 st	40-95	15.10 15.18 (63.65) (64)	84.82 (357.09)	SO ₂	Cu(MorphcbmH) ₂ O ₂	60	Endo
				2 nd	165-205	16.20 16.37 (68.28) (69)	68.45 (288.17)	H ₂ , 2O ₂		199	Endo
				3 rd	205-325	39.95 39.85 (168.4) (168)	28.60 (120.40)	4 CH ₂ =CH ₂ , N ₂ , CO		270	Endo
				4 th	325-575	10.35 10.43 (43.62) (44)	18.17 (76.49)	CO ₂	CuO	-	-

Infrared spectral studies

Various IR spectral band positions for $\text{Cu}(4\text{-MPipzcbmH})_2\text{X}_2$ and $\text{Cu}(\text{MorphcbmH})_2\text{X}_2$ ($\text{X} = \text{CH}_3\text{COO}$, $\text{X}_2 = \text{SO}_4$) have been grouped into three main frequency regions: (i) bands in the region 3431-3408 cm^{-1} because of $\nu(\text{N-H})/\text{O-H}$ vibrations, (ii) bands in the region 1654- 1544 cm^{-1} due to $\nu(\text{—O—C(=O)—N})$ modes and (iii) bands in the region 436-397 cm^{-1} due to $\nu(\text{M-O})$ vibrations. Observation of infrared absorption bands for $\text{Cu}(4\text{-MPipzcbmH})_2\text{X}_2$ and $\text{Cu}(\text{MorphcbmH})_2\text{X}_2$ ($\text{X} = \text{CH}_3\text{COO}$, $\text{X}_2 = \text{SO}_4$) reveals the non-coordinating nature for acetate ion and bridging bidentate coordination for sulphate ion (i.e. $\nu_a(\text{OCO})1603$ vs $\nu_s(\text{OCO})1455$ vs $\Delta 148$; $\nu_1 970$ m $\nu_2 356$ m $\nu_3 1108$ vs, 1042 s $\nu_4 668$ s, 618 s and $\nu_a(\text{OCO}) 1558$ vs $\nu_s(\text{OCO})1407$ vs $\Delta 151$; $\nu_1 985$ m $\nu_2 460$ m $\nu_3 1137$ s, 1085 s $\nu_4 640$ s, 615 s respectively).

Fluorescence spectroscopy studies

The fluorescent spectra of complexes, viz. $\text{Cu}(4\text{-MPipzcbmH})_2\text{X}_2$, and $\text{Cu}(\text{MorphcbmH})_2\text{X}_2$, ($\text{X} = \text{CH}_3\text{COO}$ and $\text{X}_2 = \text{SO}_4$) display maximum emission wavelengths ($\lambda_{\text{em}}^{\text{max}}$) corresponding to blue light emission at 430-432 nm and 433 - 439 nm respectively, the excitation wavelength being same, i.e. 370 nm for all compounds. A comparison of $\lambda_{\text{em}}^{\text{max}}$ data of free ligands (355 nm and 352 nm respectively) and their copper(II) complexes has revealed a red shift in emission peak values upon incorporation of metal ion into ligand moiety. Such a behaviour has earlier been reported by Yan He et al.⁷ The fluorescent emission intensities (I_{em}) for free ligands, 4-MPipzcbmH and MorphcbmH are 203 a.u. and 309 a.u. respectively. A dramatic decrease in emission intensities on complex formation for $\text{Cu}(\text{MorphcbmH})_2\text{X}_2$, ($\text{X} = \text{CH}_3\text{COO}$ and $\text{X}_2 = \text{SO}_4$) has been observed to fall at 156 and 108 a.u. whereas there is increase in emission intensities on complex formation for $\text{Cu}(4\text{-MPipzcbmH})_2\text{X}_2$, ($\text{X} = \text{CH}_3\text{COO}$ and $\text{X}_2 = \text{SO}_4$) and lie at 320 and 387 a.u. respectively. (I_{em} 4-MPipzcbmH = 203 a.u. and I_{em} MorphcbmH = 309 a.u.) Furthermore, an increase in excitation intensity (I_{ex}) for above complexes i.e. 657 - 876 a.u. at $\lambda_{\text{ex}}^{\text{max}} = 370$ nm has been observed as compared to that for free ligands, i.e. 4-MPipzcbmH and MorphcbmH: $I_{\text{ex}} = 14$ and 171 a.u. respectively at $\lambda_{\text{ex}}^{\text{max}} = 290$. It has been reported that degree of fluorescence quenching increases upon complex formation with metal ions, which have lower d-orbital electron numbers.⁸ Quenching of fluorescence of ligand by transition metal ions during complex formation is a common phenomenon, which has been explained by processes, magnetic perturbation, redox-activity, and electronic energy transfer.

Mass spectral study

The mass spectrum of $\text{Cu}(4\text{-MPipzcbmH})_2(\text{CH}_3\text{COO})_2$ (Figure-5) shows the most intense (base) peak at m/z 256 corresponding to $[\text{Cu}_2(\text{CO}_2)(\text{O}_2\text{CNCH}_2\text{CH}_3)]^+$. Mass fragmentation spectrum exhibits peculiar fragments at m/z 879 (50 %), m/z 795 (25 %), m/z 720 (50 %), m/z 636 (25 %), m/z 517 (25 %), m/z 459 (75 %), m/z 418 (25 %), m/z 314 (50 %) and m/z 215 (37.5%) corresponding to ions: $[\text{Cu}_2(4\text{-MPipzcbmH})_3(4\text{-MPipzcbm})(\text{CH}_3\text{COO})_3]^+$, $[\text{Cu}_2(4\text{-MPipzcbmH})_3(\text{O}_2\text{CNH})(\text{CH}_3\text{COO})_3]^+$, $[\text{Cu}_2(4\text{-MPipzcbmH})_2(\text{CO}_2)(4\text{-MPipzcbm})(\text{CH}_3\text{COO})_2]^+$, $[\text{Cu}_2(4\text{-MPipzcbmH})_2(\text{CO}_2)(\text{O}_2\text{CNH})(\text{CH}_3\text{COO})_2]^+$, $[\text{Cu}_2(4\text{-MPipzcbmH})(\text{CO}_2)(4\text{-MPipzcbm})(\text{CH}_3\text{COO})]^+$, $[\text{Cu}_2(4\text{-MPipzcbmH})(\text{CO}_2)(\text{O}_2\text{CNCH}_2\text{CH}_3)(\text{CH}_3\text{COO})]^+$, $[\text{Cu}_2(4\text{-MPipzcbmH})(\text{CO}_2)_2(\text{CH}_3\text{COO})]^+$, $[\text{Cu}_2(4\text{-MPipzcbm})(\text{CO}_2)]^+$ and $[\text{Cu}_2(\text{CO}_2)]^+$ respectively.

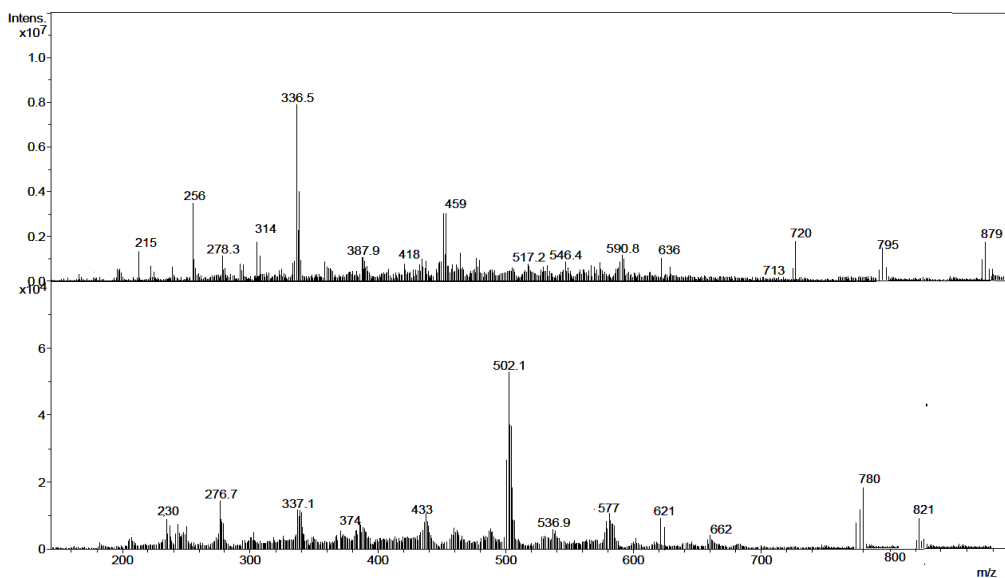


Figure-5 Mass spectra of $\text{Cu}(4\text{-MPipzcbmH})_2(\text{CH}_3\text{COO})_2$

Magnetic study

For 4-MPipzcbmH and MorphcbmH complexes of copper(II), viz. $\text{Cu}(\text{L})_2\text{X}_2$ (L = 4-MPipzcbmH, MorphcbmH and $\text{X} = \text{CH}_3\text{COO}$ and $\text{X}_2 = \text{SO}_4$) magnetic moment values at room temperature have been observed to lie in the range 1.87- 1.79 B.M. The values are indicative of the presence of one unpaired electron per copper(II) ion. Due to spin-orbit coupling magnetic moment values are higher than the spin-only value. Average magnetic moment of copper(II) complexes is not sensitive to stereochemistry. Magnetic anisotropy of the complexes is large and depends on nature of ligand fields surrounding the metal ion. For copper(II) carbamates, viz. $\text{Cu}(\text{4-MPipzcbmH})_2(\text{CH}_3\text{COO})_2$, $\text{Cu}(\text{MorphcbmH})_2(\text{CH}_3\text{COO})_2$ and $\text{Cu}(\text{4-MPipzcbmH})_2\text{SO}_4$, $\text{Cu}(\text{MorphcbmH})_2\text{SO}_4$ [CuO_4X_2] ($\text{X} = \text{CH}_3\text{COO}$ and $\text{X}_2 = \text{SO}_4$) type of chromophore could be assigned on the basis of FTIR and ESMS studies thereby suggesting distorted tetragonal or distorted octahedral stereochemistry around copper(II) ion. Distorted octahedral, tetragonal and planar structures of complexes around copper(II) ion, have also been complimented from the observed range of magnetic moment values (1.87- 1.79B.M.) , For copper(II) carbamates under study, magnetic moment values correspond to those of other dinuclear copper(II) complexes in which spin-spin exchange interaction between two metal ions has been proposed and studied in detail^{9,10}.

Electronic spectra

In DMSO solution electronic absorption spectra of 4-MPipzcbmH complexes of copper(II), viz. $\text{Cu}(\text{4-MPipzcbmH})_2\text{X}_2$ ($\text{X} = \text{CH}_3\text{COO}$ and $\text{X}_2 = \text{SO}_4$) exhibit two bands in the regions: Band I, 14084-14367 and 14580 - 14980 cm^{-1} and Band II , 28571 and 27834 cm^{-1} . For copper(II) MorphcbmH complexes, viz. $\text{Cu}(\text{MorphcbmH})_2\text{X}_2$ ($\text{X} = \text{CH}_3\text{COO}$ and $\text{X}_2 = \text{SO}_4$) bands have been observed to lie in the range: Band I, 13927-14084 and 13123 - 13333 cm^{-1} and Band II, 28735 and 28571 cm^{-1} . Band I is considered to contain electronic transitions $d_{xy} \rightarrow d_{x^2-y^2}$ and $(d_{xz}, d_{yz}) \rightarrow d_{x^2-y^2}$ for copper(II) ion in tetragonally distorted octahedral environments. Band II which appears around 27834- 28735 cm^{-1} is assigned to L→M charge transfer transition $2p_\pi \rightarrow (d_{x^2-y^2})$.

X-ray diffraction studies

PXRD pattern of $\text{Cu}(\text{MorphcbmH})_2(\text{CH}_3\text{COO})_2$ (Figure-6) exhibits sharp peaks with low value of full width at half maximum (FWHM) thus indicating their crystalline nature.^{11,12} Using Debye-Scherrer equation^{11,12} XRD crystallite sizes corresponding to a value of full width at half maximum (FWHM) for six peaks of high intensity at respective θ values were calculated and the mean value was found to be 5.71 nm. The data (Table-2) shows that larger the crystallite size of the sample, the sharper is the peak, i.e. decrease in FWHM on the XRD pattern. The tabular data for $\text{Cu}(\text{MorphcbmH})_2(\text{CH}_3\text{COO})_2$, is in good agreement with that for the reported crystalline complexes, carbamates and agriculturally active organic compounds.¹³

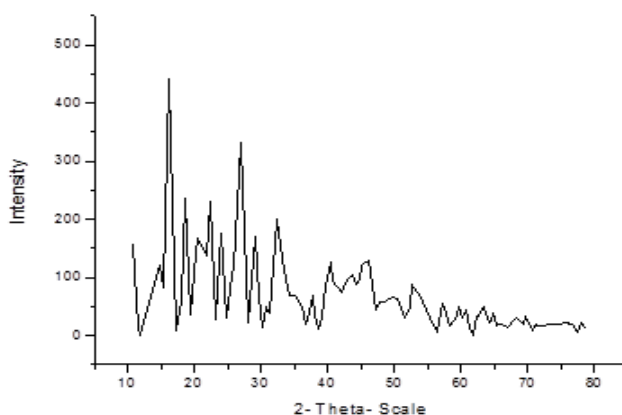


Figure -6 Powder XRD of $\text{Cu}(\text{MorphcbmH})_2(\text{CH}_3\text{COO})_2$

Table -2 XRD data of $\text{Cu}(\text{MorphcbmH})_2(\text{CH}_3\text{COO})_2$

Cu(MorphcbmH) ₂ (CH ₃ COO) ₂					
Sr.No..	d Spacing	2θ	Relative Intensity %	FWHM	Dp (nm)
1.	5.529	16.029	93.82	0.344	4.24
2.	3.305	26.973	70.19	0.196	7.58
3.	4.757	18.651	49.99	0.295	4.97
4.	3.979	22.342	49.15	0.246	6.00
5.	2.764	32.386	42.51	0.196	7.70
6.	3.696	24.077	37.19	0.393	3.77

Cyclic voltammetric study

Cyclic voltammograms (10^{-3} M DMSO solutions) of $\text{Cu}(4\text{-MPipzcbmH})_2\text{X}_2$ and $\text{Cu}(\text{MorphcbmH})_2\text{X}_2$ ($\text{X}=\text{CH}_3\text{COO}$ and $\text{X}_2=\text{SO}_4$) were recorded in presence of supporting electrolyte, KCl (10^{-1}M) with scan rate 100 mVs^{-1} and the potential range between -2.0 to 2.0V . Figure-7 shows cyclic voltammogram of $\text{Cu}(\text{MorphcbmH})_2(\text{CH}_3\text{COO})_2$. The complexes $\text{Cu}(\text{L})_2\text{X}_2$ ($\text{X}=\text{CH}_3\text{COO}$ and $\text{X}_2=\text{SO}_4$ and $\text{L} = 4\text{-MPipzcbmH}$ and MorphcbmH) show well-defined redox process corresponding to the formation of the $\text{Cu}(\text{II})/\text{Cu}(\text{III})$ couple with anodic peak in the range, $E_{\text{pa}} = 0.38\text{-}0.88\text{ V}$ and the associated cathodic peak in range $E_{\text{pc}} = 0.16\text{-}0.83\text{V}$. This couple is found to be reversible with $\Delta E = -0.08\text{-}0.22\text{ V}$ and the ratio of anodic to cathodic peak currents, $I_{\text{pa}}/I_{\text{pc}} = 0.88\text{-}1.25$ corresponding to a simple one-electron process.¹⁴ Range of potential values of CV study for copper(II) complexes is well in agreement with that of literature data.¹⁵

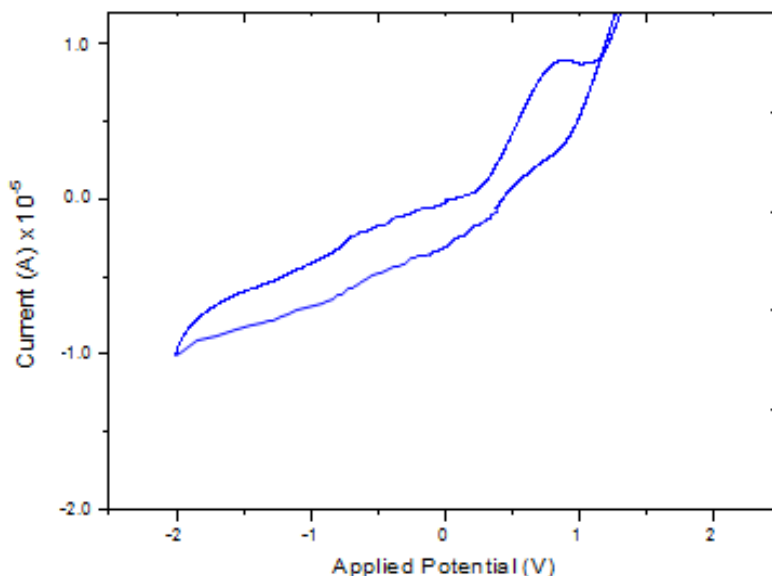


Figure -7: Cyclic Voltammogram of $\text{Cu}(\text{MorphcbmH})_2(\text{CH}_3\text{COO})_2$

Lipase activity assay

Compounds $\text{Cu}(4\text{-MPipzcbmH})_2\text{X}_2$ and $\text{Cu}(\text{MorphcbmH})_2\text{X}_2$ ($\text{X}=\text{CH}_3\text{COO}$ and $\text{X}_2=\text{SO}_4$) were also tested for the lipase enzyme (steapsin) activity at different incubation times between 0 to 70 minutes. Results (Table-3) show that the activity of the lipase enzyme gets retarded in presence of the newly synthesized copper(II) compound of 4-MPipzcbmH and MorphcbmH. The activity of the lipase enzyme is maximum at zero minute ($26.86\text{-}31.65\text{ }\mu\text{ mol/ml/min}$). When we add one milligram of compound to the lipase enzyme, then after 10 minutes its activity decreases ($2.582 - 3.044\text{ }\mu\text{ mol/ml/min}$). After 30,50 and 70 minutes the lipase enzyme activity further decreases as 0.823 to $1.286\text{ }\mu\text{ mol/ml/min}$, 0.449 to $1.286\text{ }\mu\text{ mol/ml/min}$ and 0.258 to $0.968\text{ }\mu\text{ mol/ml/min}$ respectively (Table-3). This shows that in presence of newly synthesized compounds, the activity of the lipase enzyme decreases with increase of time. Hence 4-MPipzcbmH, MorphcbmH and its copper(II) compounds retard the lipase enzyme activity. The decrease in lipase activity with time is due to fact that carbamate compounds block the active site of the lipase enzyme.

Table -3 Effect of 4-MPipzcbmH and MorphcbmH Complexes of Copper(II) on Lipase Activity ($\mu\text{ mol/ml/min}$).

Chemical Compound	Lipase Activity 0 min	Lipase Activity 10 min	Lipase Activity 30 min	Lipase Activity 50 min	Lipase Activity 70 min
$\text{Cu}(4\text{-MPipzcbmH})_2\text{SO}_4$	27.07	2.621	0.823	0.449	0.258
$\text{Cu}(4\text{-MPipzcbmH})_2(\text{CH}_3\text{COO})_2$	26.86	2.582	0.858	0.501	0.345
$\text{Cu}(\text{MorphcbmH})_2\text{SO}_4$	28.33	2.765	0.923	0.678	0.569
$\text{Cu}(\text{MorphcbmH})_2(\text{CH}_3\text{COO})_2$	31.65	3.044	1.286	1.286	0.968

References

- [1]. Chaturvedi, D. *Tetrahedron* 2012, 68, 15. (b) Kuhr, R. J.; Dorough, H. W. *Carbamate Insecticides: Chemistry, Biochemistry and Toxicology*; CRC Press: Cleveland, OH, 1976.
- [2]. Hen, N.; Bialer, M.; Yagen, B. *J. Med. Chem.* 2012, 55, 2835. (b) Niphakis, M. J.; Johnson, D. S.; Ballard, T. E.; Stiff, C.; Cravatt, B. F. *ACS Chem. Neurosci.* 2012, 3, 418. (c) Chang, J. W.; Nomura, D. K.; Cravatt, B. F. *Chem. Biol.* 2011, 18, 476. (d) Fuchs, M.; Koszelewski, D.; Tauber, K.; Kroutila, W.; Fabere, K. *Chem. Commun.* 2010, 46, 5500. (e) Wienstock, M.; Bejar, C.; Wang, R. H. *J. Neural Transm. Suppl.* 2000, 60, 157.
- [3]. Li, J.; Kornhaab, C.; Ackermann, L. *Chem. Commun.* 2012, 48, 11343. (b) Quasdorf, K. W.; Finch, A. A.; Liu, P.; Silberstein, A. L.; Komaromi, A.; Blackburn, T.; Ramgren, S. D.; Houk, K. N.; Snieckus, V.; Garg, N. K. *J. Am. Chem. Soc.* 2011, 133, 6352. (c) Riggs, J. C.; Singh, K. J.; Yun, M.; Collum, D. B. *J. Am. Chem. Soc.* 2008, 130, 13709. (d) Greene, T. W.; Wuts, P. G. M. *Protective Groups in Organic Synthesis*, 4th ed.; Wiley: New York, 2007, 419. (e) Snieckus, V. *Chem. Rev.* 1990, 90, 879.
- [4]. (a) Kreye, O.; Wald, S.; Meier, M. A. R. *Adv. Synth. Catal.* 2013, 355, 81. (b) Yoshimura, A.; Luedtke, M. W.; Zhdankin, V. V. *J. Org. Chem.* 2012, 77, 2087. (c) Lebel, H.; Leogane, O. *Org. Lett.* 2006, 8, 5717. (d) Pasguato, L.; Modena, G.; Cotarca, L.; Delgu, P.; Mantovami, S. *J. J. Org. Chem.* 2000, 65, 8224. (e) Majer, P.; Randad, R. S. *J. Org. Chem.* 1994, 59, 1937.
- [5]. (a) Takeda, Y.; Okumura, S.; Tone, S.; Sasaki, I.; Minakata, S. *Org. Lett.* 2012, 14, 4874. (b) Padiya, K. J.; Gavade, S.; Kardile, B.; Tiwari, M.; Bajare, S.; Mane, M.; Gaware, V.; Varghese, S.; Harel, D.; Kurhade, S. *Org. Lett.* 2012, 14, 2814. (c) Yang, X.; Zhang, Y.; Ma, D. *Adv. Synth. Catal.* 2012, 354, 2443. (d) Shang, J.; Liu, S.; Ma, X.; Lua, L.; Deng, Y. *Green Chem.* 2012, 14, 2899. (e) Ca, N. D.; Gabriele, B.; Ruffolo, G.; Veltri, L.; Zanetta, T.; Costa, M. *Adv. Synth. Catal.* 2011, 353, 133. (f) Shi, F.; Deng, Y. *Chem. Commun.* 2001, 443.
- [6]. (a) Kalia, S.B.; Kumar, R. Indian patent app. 1729/DEL/2013 Official journal of the patent office, date-06/10/2013. (b) Kalia, S.B.; Kaushal, G.; Lumba, K.; Priyanka. *J. Therm. Anal. Calorim.*, 2008, 91(2), 609-613.
- [7]. Yan, H.; Zhong, C.; Zhou, Y.; Zhang, H. *J. Chem. Sci.* 2009, 121, 407-412.
- [8]. Onal, Z.; Zengin, H.; Sonmez, M. *Turk. J. Chem.* 2011, 35, 905-914.
- [9]. Boguslavskii, E.G.; Shklyayev, A.A. *Russian Chemical Bulletin.* 1982, 31(6), 1159-1163.
- [10]. Boguslavskii, E.G.; Shklyayev, A.A.; Maksimov, N.G.; Alaudinova, Z.M.; Kolomnikov, I.S.; Anufreko, V.F. *Russian Chemical Bulletin*, 1980, 29(6), 857-859.
- [11]. Goldstein, G. I.; Newbury, D. E.; Echlin, P.; Joy, D. C.; Fiori, C.; Lifshin, E. *Scanning electron microscopy and x-ray microanalysis*. New York, Plenum Press. 1981.
- [12]. Tomar, R.; Sharma, P. *Ind. J. Chem.*, 2006, 45(A), 1400-1404.
- [13]. Rafel, I.; Heidi Emilia, S.; Mathias, B.; Marco, K.; Peter, E. *US Patent App.* 20100113543, 2010.
- [14]. Shirin, Z.; Mukherjee, R. M. *Polyhedron*, 1992, 11, 2625.
- [15]. Raman, N.; Ravichandran, S.; Thangaraja, C. *J. Chem. Sci.* 2004, 116(4), 215-219.